

Research Article

Open Access



AI-driven design of fluorine-free polymers for sustainable and high-performance anion exchange membranes

William Schertzer¹, Shivank Shukla¹, Abhishek Sose¹, Reanna Rafiq¹, Mohammed Al Otmi², Janani Sampath², Ryan P. Lively³, Rampi Ramprasad^{1*} 

¹Department of Materials Science and Engineering, Georgia Institute of Technology, Atlanta, GA 30332, USA.

²Department of Chemical Engineering, University of Florida, Gainesville, FL 32611, USA.

³Department of Chemical and Biomolecular Engineering, Georgia Institute of Technology, Atlanta, GA 30329, USA.

* **Correspondence to:** Dr. Rampi Ramprasad, Department of Materials Science and Engineering, Georgia Institute of Technology, 771 Ferst Drive NW, Atlanta, GA 30332, USA. E-mail: rampi.ramprasad@mse.gatech.edu

How to cite this article: Schertzer, W.; Shukla, S.; Sose, A.; Rafiq, R.; Otmi, M. A.; Sampath, J.; Lively, R. P.; Ramprasad, R. AI-driven design of fluorine-free polymers for sustainable and high-performance anion exchange membranes. *J. Mater. Inf.* 2025, 5, 5. <https://dx.doi.org/10.20517/jmi.2024.69>

Received: 8 Nov 2024 **First Decision:** 3 Dec 2024 **Revised:** 16 Dec 2024 **Accepted:** 26 Dec 2024 **Published:** 16 Jan 2025

Academic Editors: Xingjun Liu, Runhai Ouyang, Rika Kobayashi **Copy Editor:** Pei-Yun Wang **Production Editor:** Pei-Yun Wang

Abstract

As global demand for clean energy increases, fuel cells have emerged as a key technology for sustainable power generation. Anion exchange membrane (AEM) fuel cells offer a more economical and environmentally friendly alternative to the popular proton exchange membrane (PEM) fuel cells, which rely on fluorinated polymers and also use expensive platinum group catalysts. However, designing high-performance AEMs is challenging because of the need to balance conflicting material properties. In this study, we employ machine learning to accelerate the design of fluorine-free copolymers for AEMs, focusing on known monomer chemistries. By training models on AEM data from the literature, we predicted key properties, namely, hydroxide ion conductivity, water uptake (WU), and swelling ratio (SR). Screening 11 million novel copolymer candidates using predictive models and heuristic filters, we identified more than 400 promising fluorine-free copolymer candidates with predicted OH⁻ conductivity greater than 100 mS/cm, WU below 35 wt%, and SR below 50%. This computational approach to AEM design could contribute to developing more efficient and sustainable AEM fuel cells for various energy applications.

Keywords: Anion exchange membrane, fuel cells, anion conductivity, water uptake, swelling, materials informatics, high-throughput polymer design



© The Author(s) 2025. **Open Access** This article is licensed under a Creative Commons Attribution 4.0 International License (<https://creativecommons.org/licenses/by/4.0/>), which permits unrestricted use, sharing, adaptation, distribution and reproduction in any medium or format, for any purpose, even commercially, as long as you give appropriate credit to the original author(s) and the source, provide a link to the Creative Commons license, and indicate if changes were made.



INTRODUCTION

Fuel cells have emerged as a promising solution to the global energy crisis. A large body of prior research has focused on advances in proton exchange membrane (PEM) fuel cells^[1,2]; however, several factors hinder their widespread adoption. Fluorinated polymers and platinum catalysts used in PEMs to prevent corrosion are costly and environmentally harmful^[1,3,4], and effective water and carbon monoxide management is also crucial to avoid rapid degradation of performance^[1,5,6].

Over the past two decades, anion exchange membrane (AEM) fuel cells have emerged as promising alternatives to PEM fuel cells. AEMs utilize hydroxide ions for ion transport and thus operate in an alkaline environment, which offers several advantages over the acidic environments present in PEMs, as illustrated in [Figure 1A](#). Notably, because AEMs operate in alkaline environments, expensive fluorinated polymers and other acid-tolerant materials are no longer required, potentially leading to significant reductions in material costs compared to traditional PEMs. [Figure 1B](#) shows the chemical structures of Nafion and Sustainion, the leading PEM and AEM materials, respectively. Although the prospect of non-fluorinated membranes is exciting, AEMs face major challenges, including low ionic conductivity, limited chemical/alkaline stability, and mechanical integrity issues. These limitations stem primarily from the conduction of anions - which have inherently lower diffusion constants compared to protons - and excessive water adsorption and swelling^[1,3].

The United States Department of Energy has set ambitious goals for AEM performance over the next five years, namely: hydroxide conductivity of at least 100 mS/cm, swelling ratio (SR) of no more than 50%, durability of 25,000 h with no more than 10% loss in current density, and a cost no greater than \$40/kW. These goals were identified with the hope of designing polymers that can outperform PEMs in energy generation capability and long-term stability without the need for halogenated backbones or functional groups, with fluorine being the most commonly used halogen to impose ionic conductivity and chemical stability^[4,7].

One solution to increase conductivity is to enhance the ion exchange capacity (IEC), defined as the total number of active sites responsible for ion exchange in the polymer electrolyte membrane (reported in units of meq/g). However, this often leads to mechanical instability due to excessive water uptake (WU)-induced swelling, and chemical instability due to the elimination of charged groups under alkaline environments^[2,3,8]. AEMs are also prone to rapid chemical and mechanical degradation^[6,9]. A common approach for increasing stability is the addition of fluorinated groups, but there is a strong push to move away from fluorinated polymers amid environmental health concerns^[3,5-7]. The primary challenge is thus to develop an AEM that combines high ionic conductivity with strong mechanical and chemical stability across a range of temperatures and humidities without the use of fluorinated chemistries, replicating the benefits of PEMs while significantly reducing the cost and environmental impact of using fluorinated polymers. Achieving this balance has proven extremely difficult due to conflicting property requirements. We wish to maximize hydroxide conductivity while limiting the WU and SR, but as indicated in [Figure 2](#), there exists a positive correlation between these properties of interest, making this a non-trivial task. Additionally, because of its high alkaline stability, fluorine is present in ~25% of the top-performing candidates (OH^- conductivity ≥ 100 mS/cm) that were found in the literature. This highlights the difficulty of designing state-of-the-art polymers for AEMs that contain no fluorine.

AEM performance is intricately linked to several factors, including WU, SR, temperature, relative humidity (RH), and IEC. RH, expressed as a percentage, measures the level of environmental humidity. WU and SR, both known to correlate with anion conductivity and mechanical stability, are frequently reported alongside

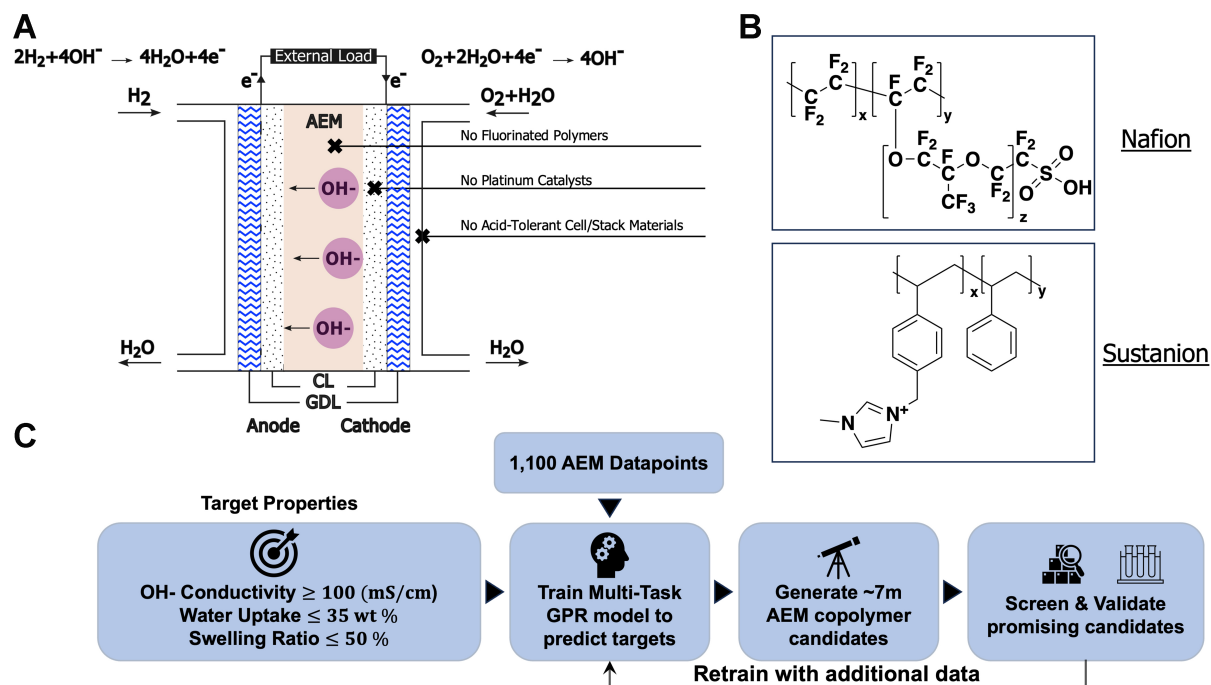


Figure 1. Overview of the design and benefits of AEMs compared to PEMs. (A) Schematic of an AEM fuel cell, highlighting key advantages over PEMs, such as reduced cost and the elimination of fluorinated polymers; (B) Chemical structures of Nafion (the most commonly used PEM material) and Sustanion (a representative AEM material), demonstrate the shift away from fluorine-based chemistry; (C) Workflow of the AI-driven design process for novel AEMs, including target property identification, data curation, ML model training, candidate generation, screening, and optimization based on active learning. AEMs: Anion exchange membranes; PEMs: proton exchange membranes; ML: machine learning.

or instead of direct mechanical properties. WU is defined as the amount of water a polymer sample can absorb at full saturation, expressed as a weight percentage of the dry polymer as in:

$$\text{WU} = \frac{\text{weight of wet polymer} - \text{weight of dry polymer}}{\text{weight of dry polymer}} \times 100\% \quad (1)$$

Similarly, SR refers to the increase in volume of a polymer sample when it transitions from a dry state to full saturation (i.e., 100% RH or liquid water conditions), expressed as a percentage of the initial dry volume as in:

$$\text{SR} = \frac{\text{volume of wet polymer} - \text{volume of dry polymer}}{\text{volume of dry polymer}} \times 100\% \quad (2)$$

Anion conductivity, WU, and SR are evaluated across various temperatures, RH levels, and IEC values. Some studies also investigate membrane properties before and after immersion in solvents of varying concentrations over several days. This time-dependent behavior is crucial for understanding the long-term stability of AEMs. However, due to data limitations, this aspect will be addressed in future research. Conductivity in AEMs follows an Arrhenius relationship, with the natural log of conductivity showing a decreasing linear trend with the inverse of temperature^[10-12] while WU and SR show a linear relationship

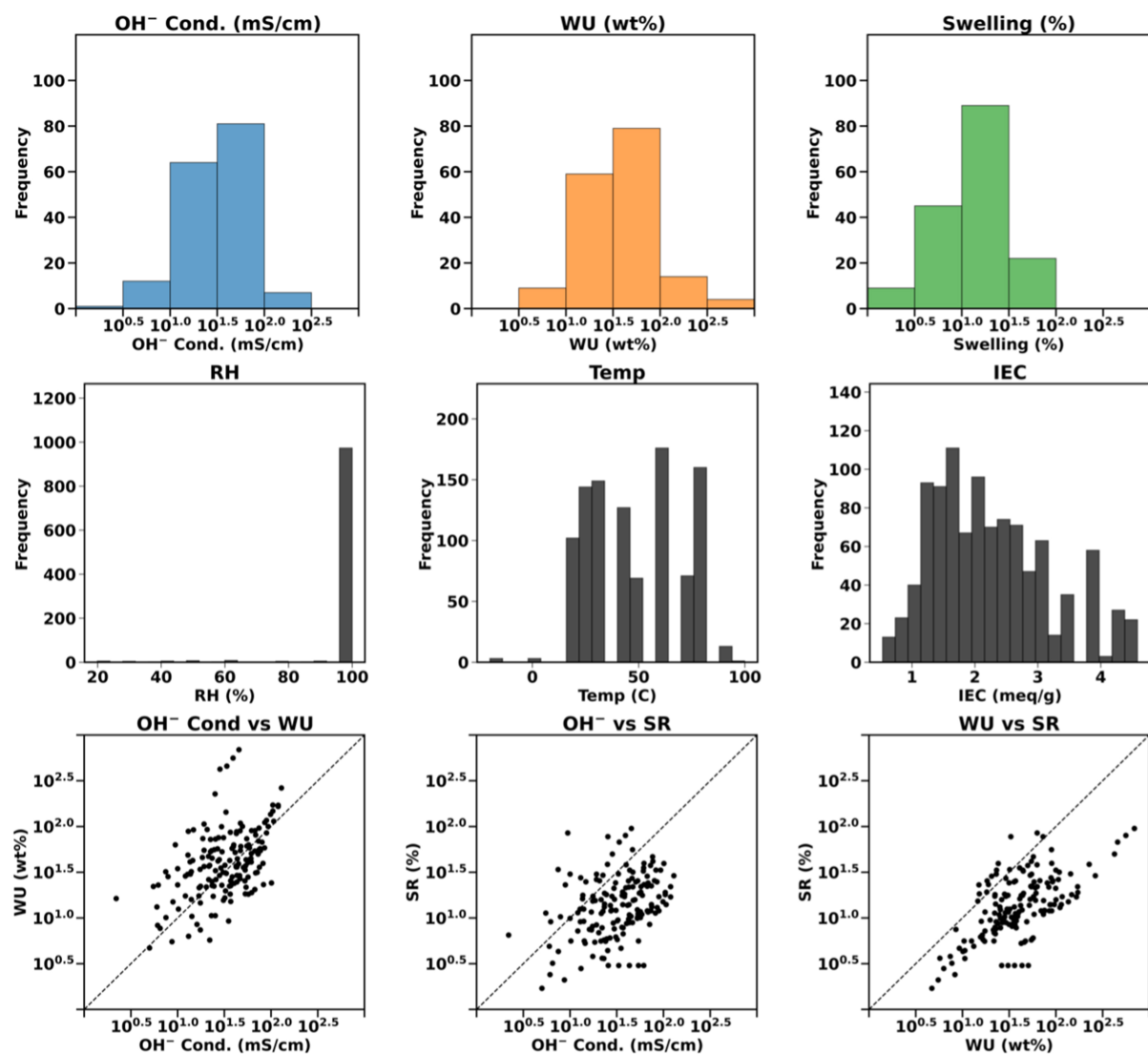


Figure 2. Top: Distribution of the observed data for each of the target properties (OH⁻ Conductivity, equilibrium WU, and SR), Middle: Distribution of input variables used in the machine learning model: RH (%), measurement temperature (°C), and IEC (meq/g), Bottom: scatter plots for each pair of properties, highlighting the correlation between them. WU: Water uptake; SR: swelling ratio; RH: relative humidity; IEC: ion exchange capacity.

with temperature and RH^[12]. AEMs typically operate under conditions of 100% RH, representing complete saturation with liquid water, to ensure a continuous flow of water at the electrodes. The IEC can be adjusted by varying the monomer ratio within a copolymer.

IEC is a crucial descriptor for modeling AEMs. However, experimental IEC, which differs from theoretical IEC due to system effects, cannot be determined for candidate polymers without synthesizing them^[13-15]. Theoretical IEC refers to the maximum number of ions that a material can theoretically exchange and assumes that all exchange sites are equally accessible, there are no material imperfections, and that environmental (temperature, pH) and kinetic effects are negligible. This limitation means that, for candidate polymers, we have no direct knowledge of the experimental IEC. Fortunately, as shown in [Figure 3](#), theoretical IEC is qualitatively similar to experimental IEC, even when the measured IEC is twice that of theoretical IEC, as in the case of quaternized poly(phenylene) oxide (QPPO)-x. Theoretical IEC can

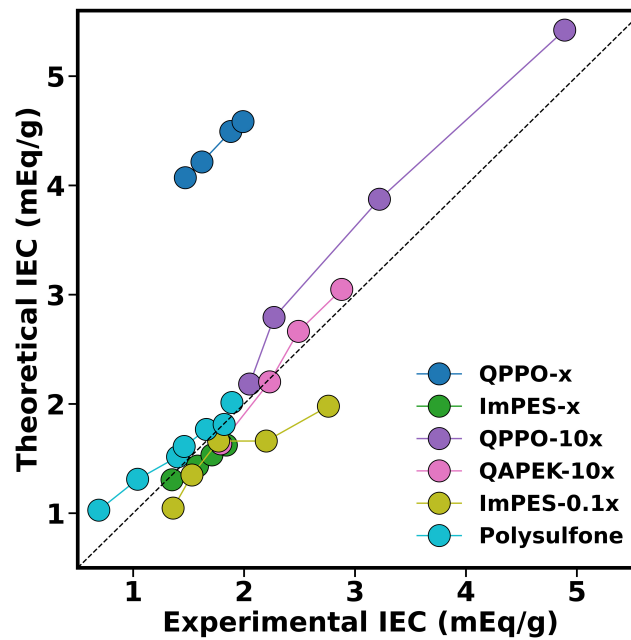


Figure 3. Comparison of theoretical IEC vs. experimental IEC for various AEM polymers. Theoretical IEC, calculated from the polymer's chemical structure, is generally consistent with experimental values. This correlation is essential for predicting the performance of candidate polymers without the need for experimental synthesis. The plot includes various polymer classes: QPPO-x, ImPES-x, QPPO-10x, QAPEK-10x, ImPES-0.1x, and Polysulfone, each represented by different colors and markers. The dashed line represents the ideal case where theoretical and experimental IEC are equal ($y = x$). IEC: Ion exchange capacity; AEM: anion exchange membrane; QPPO: quaternized poly(phenylene) oxide.

be calculated from the chemical structure of the polymer alone; thus, for candidate polymers, we rely on theoretical IEC, which is calculated by:

$$\text{Theoretical IEC} = \frac{\text{number of active ion exchange sites (meq)}}{\text{molecular weight of polymer repeat unit (g)}} \times 100\% \quad (3)$$

Although both vehicular and Grotthuss transport influence anion conduction, understanding the relative contributions of these two transport mechanisms is an ongoing area of research^[10,11]. The dependence of vehicular ion transport on water in hydrated polymer systems is well-established, and the characterization of water channels within the AEM is crucial.

Ion-containing polymer membranes often exhibit microphase segregation, leading to the formation of water channels, particularly when monomers feature extended side chains. These water channels promote anion conduction, but excessive WU compromises the mechanical integrity of the AEM through unwanted swelling^[16,17]. Anion conductivity, WU, and SR are interrelated but independently affected by morphology and polymer chemistry, exhibiting complex inherent correlations with chemistry, temperature, and RH^[18].

Given these challenges, this problem may be well-suited for an informatics-based approach, which is beginning to show promise^[19]. Machine learning (ML) models can rapidly evaluate vast lists of potential materials, filtering and identifying the most promising candidates for experimental validation. This approach has the potential to accelerate the material discovery process, as extensively reviewed^[20]. In

previous work, we explored a large space of PEMs using ML models for proton conductivity, WU, and several other properties^[21].

In the present study, we leverage ML to develop predictive models based on curated AEM data from the literature, aiming to design robust polymers with high anion conductivity, low WU, and low SR. The informatics-based approach, outlined in [Figure 1C](#), comprises four distinct steps. First, we identify critical properties and their optimal desired values based on design of experiments (DOE) and literature guidelines. Our objective is to identify innovative copolymers that exhibit hydroxide conductivity greater than 100 mS/cm, equilibrium WU less than 35 wt%, and equilibrium SR below 50%, with SR and WU serving as proxies for degradation and indicators of anion conductivity. We use WU and SR as proxies for stability because of data scarcity and because polymers with lower water adsorption are less likely to experience degradation due to unwanted swelling. Next, we train ML models to predict these key properties using measured property data curated from the literature. Then, a large set of candidate copolymers built using known comonomers was generated to define the search space. Finally, we use the ML models to predict the key properties of these candidates and screen them to find the optimal candidates for further exploration. Future work will address mechanical and chemical stability directly by incorporating time-dependent conductivity and mechanical property retention data into a holistic AEM dataset.

MATERIALS AND METHODS

Dataset

The AEM dataset comprises approximately 1,100 data points collected from the literature, involving 108 unique monomers, including information on hydroxide conductivity, WU, and SR for polymer electrolytes^[5,22-60]. The chemical space includes copolymers; thus, we record both the chemistry information for each monomer and the relative composition of each monomer in the copolymer. For each data point, we collect an associated measurement of temperature, RH, and experimental IEC. [Figure 2](#) shows the distribution of various properties in the dataset, the correlation between each pair of properties, and the distribution of variables used as descriptors in the ML models. [Table 1](#) shows a fragment of the dataset, including its structure. The full data set and training splits are available on the [polyVERSE GitHub](#).

Feature engineering

In previous work, polymers were characterized using the Co-Polymer Genome fingerprinting scheme, which has been demonstrated to accurately model the properties of copolymers^[61]. Each monomer repeat unit is decomposed into a hierarchical feature vector, which serves as a numerical representation of the chemical building blocks. We then perform a linear combination of the fingerprint vectors of each comonomer weighted by their respective composition within the copolymer. Each fingerprint vector is concatenated with the sample temperature, RH, and IEC, as defined by Equations (1-3), respectively.

ML algorithm

The fingerprint vectors are fed through a Gaussian process regression (GPR) framework for parameter optimization which allows us to map the chemical structure and environmental conditions to the desired properties. This allows us to predict the properties of candidate polymers later. We use a radial basis function (RBF) kernel multiplied by white noise and linear kernels to train the property prediction models^[61-63].

We train both single-task (ST) and multi-task (MT) models^[61] to predict multiple properties of interest. In ST learning, each model is trained to predict only one property at a time, while in MT learning, a single model is trained to predict several properties simultaneously. To assess the predictive capabilities of both approaches, we divide the data into training and test sets in three distinct ways:

Table 1. Example snippet of the dataset used for training machine learning models in the design of AEMs

SMILES1	SMILES2	c1	c2	Temp (C)	RH (%)	IEC (meq/g)	Property	Value
Cc1cc(*)...	(*)C(C...	37	63	25	100	2.33	OH ⁻ Cond. (mS/cm)	12.1
Cc1cc(*)...	(*)C(C...	37	63	25	100	2.33	WU (wt%)	17.4
Cc1cc(*)...	(*)C(C...	37	63	25	100	2.33	SR (%)	7.2

The dataset includes copolymer repeat unit SMILES strings, monomer compositions, and associated experimental property measurements. AEMs: Anion exchange membranes; RH: relative humidity; IEC: ion exchange capacity; WU: water uptake; SR: swelling ratio.

1. Polymer split (PS): The test set contains a set of monomers that are completely absent in the training set. This simulates the prediction of properties for chemistries that are unseen by the training dataset.
2. Composition split (CS): The test set is composed of data points with monomers that are present in the train set but with unique combinations of monomers and compositions. This simulates the interpolation of the monomers captured in the training set to novel copolymers.
3. Temperature split (TS): The test set consists of data points from identical chemistries to a subset of the training data, but has a different temperature measurement and, consequently, recorded property values. This scenario tests the model's capacity to predict properties for copolymer compositions and monomers seen previously under unseen temperature conditions.

Finally, a production model was trained on the full dataset to make predictions for the candidate set. To ensure statistical significance, all models were evaluated using five-fold cross-validation in five seed-splitting randomizations and five different train-test ratios.

Candidate generation

We generate a set of novel candidates by enumerating every combination of three repeat units from our set of 108 unique monomer units with each composition in increments of 10%. Figure 4 depicts this process pictorially. This resulted in the generation of approximately 11 million candidates, including copolymers with extreme IEC values (which are impractical for AEM materials; low IEC leads to low ionic conductivity and high IEC causes mechanical instability)^[3,8].

Further screening is performed to identify promising candidates without fluorine-containing monomers. By ensuring that our proposed candidates contain no fluorine, we impose sustainability and cost as key criteria in our polymer discovery efforts. This work is primarily motivated by our desire to discover functional polymers with no fluorine, as fluorinated polymers are known to be toxic and expensive.

RESULTS AND DISCUSSION

Model performance

The MT framework trains on datasets encompassing multiple properties, enhancing predictive performance and enabling exploration of broader chemical diversity. Unlike ST models, MT models learn shared information across related tasks, capturing correlations between properties such as hydroxide conductivity, WU, and SR.

Figure 5 shows the performance of various models across a range of train-test ratios, illustrating how MT learning improves performance for all split types and all test-train ratios, and Figure 6 presents representative instances of the different splitting methods for OH⁻ conductivity with 80% of the data in the training set. Both the ST and MT models struggled in the PS setting across all test-train ratios. Note the high root mean squared error (RMSE), low coefficient of determination (R^2), and exceptionally large error bars for all PS parity plots. These metrics highlight the difficulty of accurately and confidently predicting the

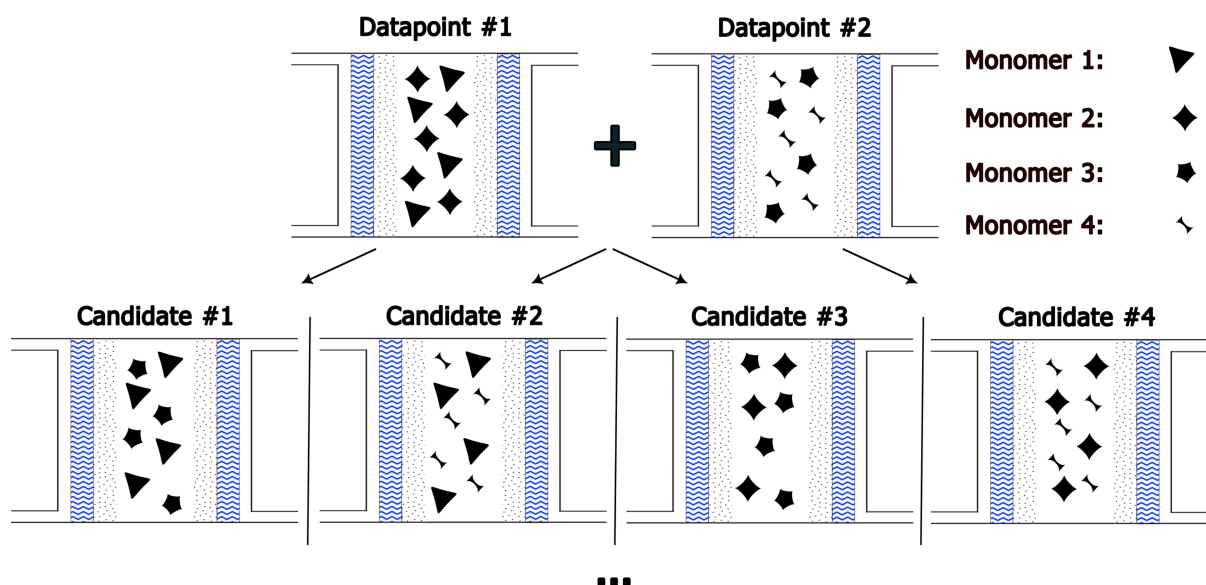


Figure 4. Illustration of the candidate generation process: unique monomer units are extracted from the training dataset and combined in various ratios to generate novel random copolymer candidates. Each candidate's composition is varied in 10% increments, resulting in a search space of approximately 11 million candidates. The copolymers are then screened based on theoretical IEC to filter for candidates with IEC values between 0.5 and 5 meq/g. The selected candidates undergo ML-based property predictions for hydroxide conductivity, WU, and SR for further screening. IEC: Ion exchange capacity; ML: machine learning; WU: water uptake; SR: swelling ratio.

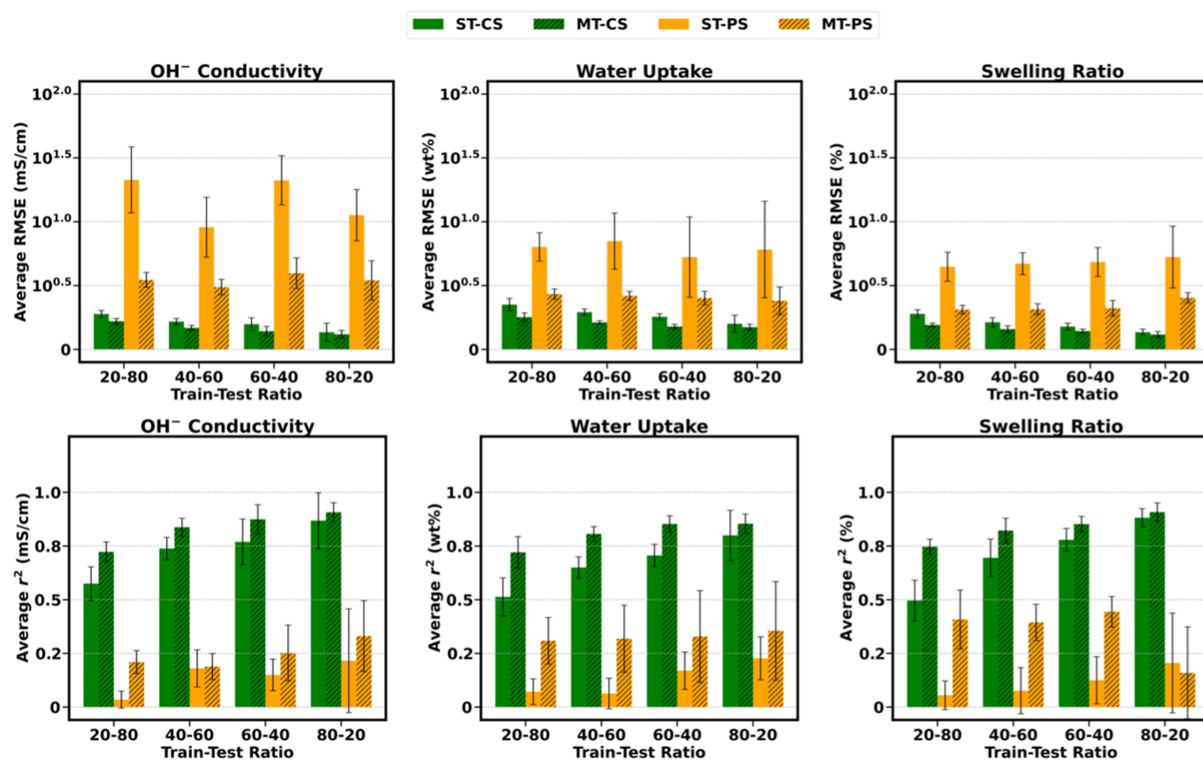


Figure 5. Average RMSE and R^2 for five random seeds at various train-test splits for each property. Green bars represent CS, and orange bars represent PS. Solid-colored bars represent ST learning, and the hashed bars represent MT models. The error bars correspond to the standard deviation across the five random seeds for each split and train-test ratio type. RMSE: Root mean squared error; R^2 : coefficient of determination; CS: composition split; PS: polymer split; ST: single-task; MT: multi-task.

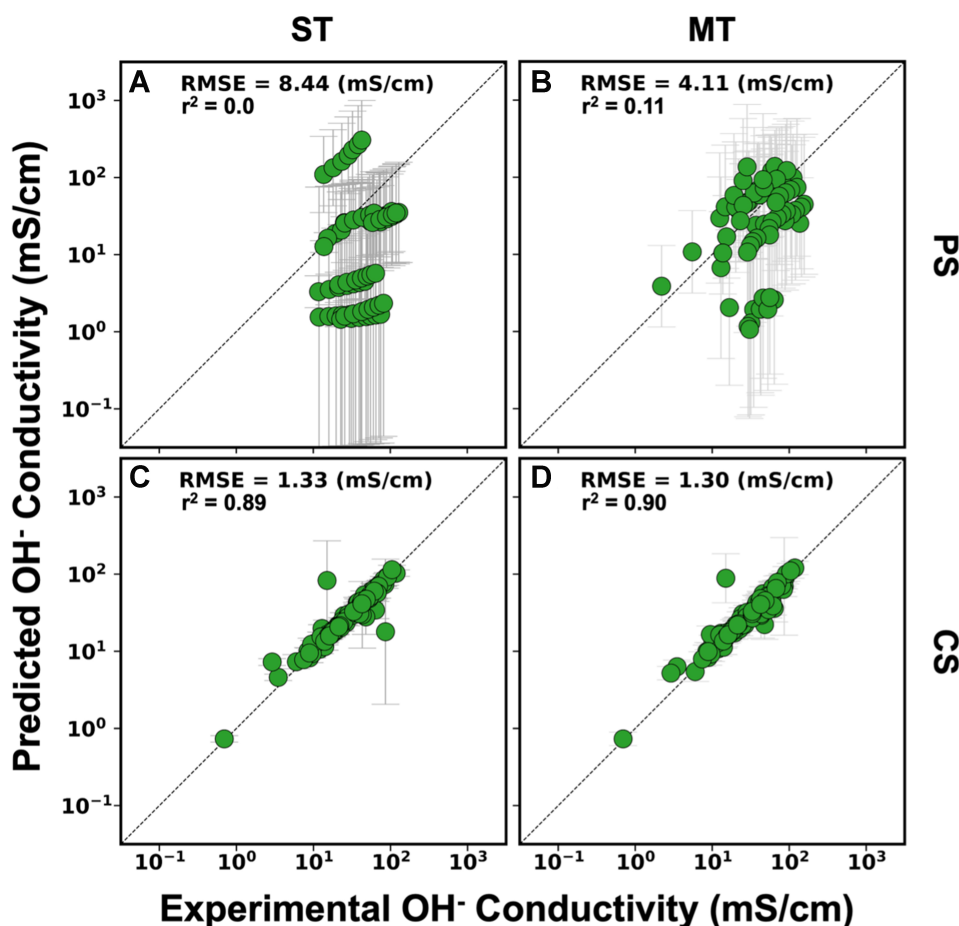


Figure 6. Comparison of predicted vs. true values of hydroxide conductivity (mS/cm) for PS and CS datasets using ST and MT models for a single instance of 80% training data and 20% testing data. (A) and (B) represent ST and MT predictions for the PS dataset, while (C) and (D) represent ST and MT predictions for the CS dataset. The diagonal dashed line indicates the ideal case in which predicted values perfectly match the true values. The RMSE and R^2 values for each model are provided, demonstrating improved predictive performance with the MT models in both the PS and CS splits. The error bars represent prediction uncertainty, highlighting the increased confidence of the MT model. PS: Polymer split; CS: composition split; ST: single-task; MT: multi-task; RMSE: root mean squared error; R^2 : coefficient of determination.

properties of novel polymers without prior examples of the corresponding chemistry (e.g., extrapolation to novel polymer classes). The MT model outperformed the ST model for all split types and test-train ratios, indicating its ability to generalize across shared structural features despite the absence of direct training examples. This suggests that augmenting the dataset with additional monomer chemistries could significantly enhance the model's extrapolative capabilities. The superior performance of the MT model implies that capturing deeper polymer structure-property relationships leads to better generalization with more comprehensive data.

Compared with the PS split, the CS, where the test set included new combinations or compositions of known monomers, represented an easier challenge because the model could rely on learned knowledge about individual monomers and their interactions. The MT model outperformed the ST model in this case as well. This is due to the ability of the MT model to leverage the shared information across tasks, allowing it to make more accurate predictions for unseen copolymer compositions by drawing on correlations between different properties. The strong performance of the model in this split demonstrates its proficiency

in interpolation within the chemical space defined by the training set, making it a valuable tool for optimizing new combinations of known monomers for improved AEM performance.

The TS, which tested the model's ability to predict properties of known chemistries at different temperatures, further showcased the advantage of MT learning. Figure 7 shows how the MT model captures the expected linear trend (Arrhenius behavior) of hydroxide conductivity slightly beyond the temperature range captured by the training dataset for three different polymers. As shown by the gray vertical dashed lines, the linear regime stretches from 275 to 400 K. This ability to predict across different temperature conditions is crucial for understanding real-world AEM performance, as operational environments in fuel cells can vary widely.

Based on the performance of the MT models across all splits, we anticipate that the final model - incorporating all curated data - will exhibit strong interpolative capabilities but currently has limited extrapolative behavior to new monomer chemistries due to the small dataset size. The superior performance of the MT model in the challenging PS suggests that increasing the size and chemical diversity of the dataset will enhance its ability to predict novel chemistries. Its robust interpolative performance in the composition and TS provides confidence in predicting the properties of new candidate copolymers composed of known monomers. As the dataset grows, we expect improvements in both extrapolation and interpolation, leading to more accurate predictions for entirely novel AEM polymer chemistries. In future work, we plan to expand our dataset to include poly(aryl piperidinium), polynorbornene, and other advanced chemistries and extend from just neat thermoplastics to also incorporating thermosets, composites, and blends.

SHapley Additive exPlanations (SHAP) analysis was used to add an element of interpretability to the ML models by identifying the most important input features. Figure 8 shows the top ten most impactful chemical features from most important (top) to least important (bottom). From the SHAP analysis, we identified temperature and IEC as having the major impact on the model output, along with certain chemical motifs such as quaternary ammonium ions, backbone toluene, and side chain length. The effect of these chemical motifs on AEM fuel cell performance should be explored in future works, with this analysis aiding in the explainable design of AEM membranes. As quaternary ammonium cations were found to be one of the most descriptive chemical features, their effect on the AEM performance needs to be thoroughly investigated.

Promising candidates and design suggestions

Our candidate set addresses the gaps in the AEM literature over the past 20 years. By enumerating all captured chemistries at various monomer ratios, we explore the full spectrum of synthesized and characterized monomer combinations. This comprehensive approach enables us to identify polymers with fine-tuned properties without compromising the synthetic feasibility.

Among the approximately 11 million candidates generated, 6.5 million did not contain fluorine. Of these, 478 candidates met all the property criteria: anion conductivity of ≥ 100 mS/cm, maximum WU of ≤ 35 wt%, and maximum SR of ≤ 50 wt%. The expected improvement (EI) for each property for each candidate was calculated using:

$$EI = (\mu(x) - f_{\text{best}} - \xi) \cdot \Phi\left(\frac{\mu(x) - f_{\text{best}} - \xi}{\sigma(x)}\right) + \sigma(x) \cdot \phi\left(\frac{\mu(x) - f_{\text{best}} - \xi}{\sigma(x)}\right) \quad (4)$$

where δ for maximization is equal to the predicted mean at x , $\mu(x)$, minus the best-observed data point, f_{best} ,

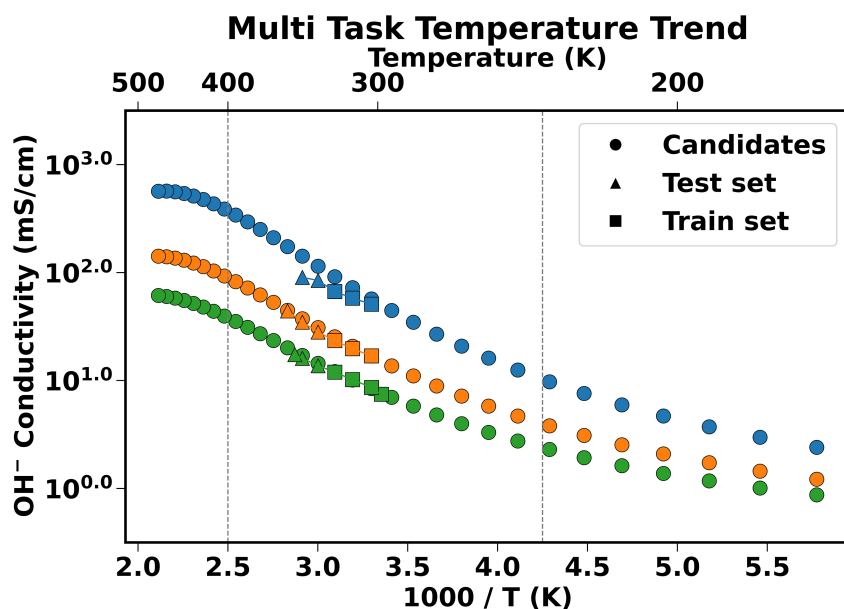


Figure 7. Predicted vs. true values of hydroxide conductivity (mS/cm) for TS using the MT model on a few representative polymers from the curated dataset, with each color representing a unique polymer. The square and triangle markers indicate the train and test set, respectively, indicating the model’s ability to predict the properties at higher temperatures given samples at lower temperatures. The circles represent the candidate polymers across a range of temperatures and are used to establish the range of acceptable property predictions. The dashed vertical lines indicate the range of acceptable temperatures used for conductivity predictions. TS: Temperature split; MT: multi-task.

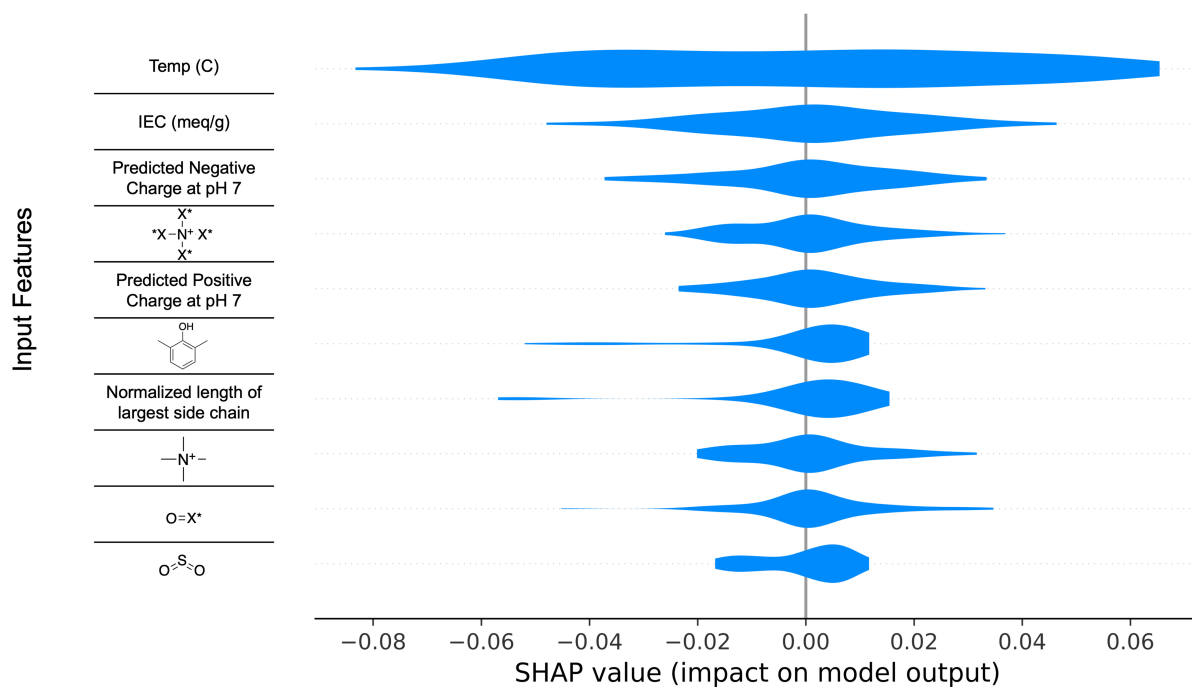


Figure 8. Top ten most important input features to the MT GPR model as identified by SHAP analysis. MT: Multi-task; GPR: Gaussian process regression; SHAP: SHapley Additive exPlanations.

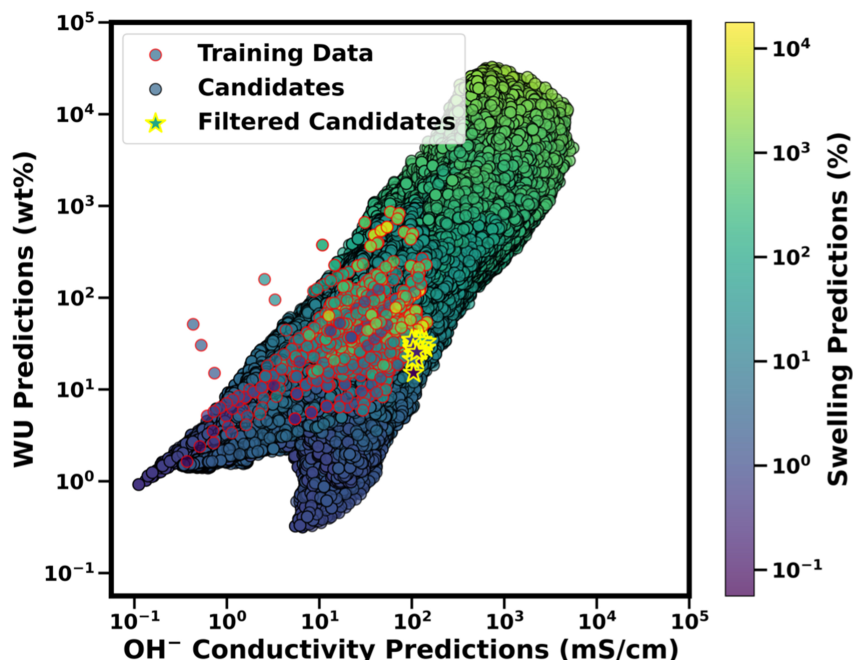


Figure 9. Predicted hydroxide conductivity (OH^- conductivity, mS/cm) vs. equilibrium WU (wt%) for the training dataset (experimental data) and the candidate copolymers (prediction data). The color map represents the predicted equilibrium SR (%), with darker shades indicating lower SRs. The star markers indicate the candidates with no fluorine that meet all ideal screening criteria: hydroxide conductivity ≥ 100 mS/cm, WU $\leq 35\%$, SR $\leq 50\%$. The figure demonstrates how the ML model identifies promising AEM candidates with optimized properties for further investigation. WU: Water uptake; SR: swelling ratio; ML: machine learning; AEM: anion exchange membrane.

and for minimization δ is equal to f_{best} minus $\mu(x)$, $\sigma(x)$ is the predicted standard deviation (error) at x , ξ is the exploration parameter that balances exploitation and exploration and is set to 0.01, Φ is the cumulative distribution function of the normal distribution, and φ is the probability density function of the normal distribution.

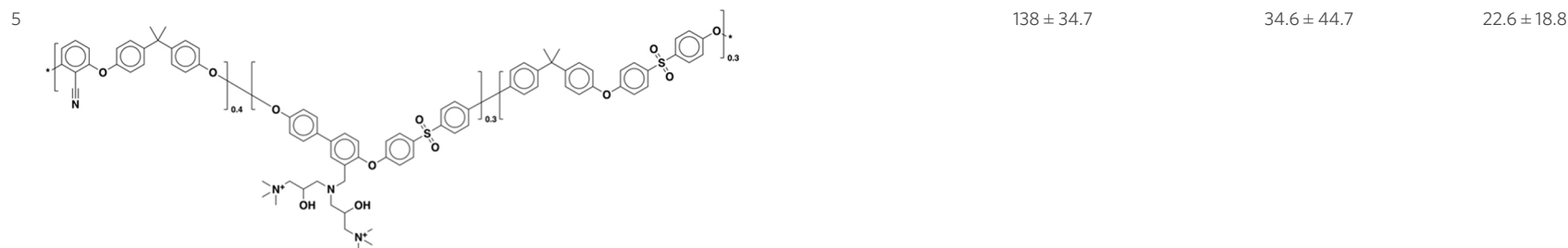
The candidates were ranked by the sum of the normalized EI across all of the properties. Figure 9 presents the predicted hydroxide conductivity, WU, and SR overlaid with the training data and the filtered candidates. As anticipated, the candidate set effectively fills gaps in the training data and, in some instances, extends the boundaries of property combinations toward more desirable outcomes. These candidates offer slight modifications to existing experimental data points while combining favorable properties of several copolymers reported in the literature. Table 2 shows the chemical structure and predicted properties of some selected candidates. Notably, the selection of candidates contains a large range of prediction uncertainties. The intended goal is to balance the exploration of unconfident chemical space with the exploitation of the comfortable chemical space. The remaining screened candidates are available on the [polyVERSE GitHub](#). We are optimistic that some of these exceptional candidates will be synthesized and validated in the future. The measurements made on these candidates can serve as valuable training data points for recursive ML model training, potentially improving the predictive performance of our models.

CONCLUSIONS

Our approach takes a significant step toward accelerating the discovery of AEM materials while illuminating the balance between polymer chemistry, morphology, performance, and stability. Although challenges persist, especially in moving beyond the limited chemical space that dominates AEM research, our method

Table 2. The chemical structure and predicted properties of a handful of top-performing copolymer candidates

#	Chemical structure	OH ⁻ Pred. (mS/cm)	WU Pred. (wt%)	SR Pred. (%)
1		101.9 ± 1.06	30.2 ± 1.1	18.6 ± 1.3
2		114.7 ± 1.94	21.2 ± 2.5	6.4 ± 3.2
3		107.8 ± 44.2	27.2 ± 57.7	14.4 ± 23.1
4		131.83 ± 34.7	27.2 ± 57.5	19.9 ± 22.9



WU: Water uptake; SR: swelling ratio.

offers an immediate pathway to identifying stable, high-conductivity polymers without relying on fluorinated monomers.

To summarize the findings and contributions presented in this work:

- Although the body of AEM data remains relatively small, it provides untapped potential for exploring the vast copolymer space, offering practical solutions for material challenges.
- Using theoretical IEC as a key descriptor in ML models, we bypass the need for synthesized samples, accelerating the screening process.
- Incorporating several properties in a MT framework empowers us to pinpoint materials that portray high hydroxide conductivity, low WU, and low SR. In the future, mechanical properties and performance under alkaline conditions should be considered to identify polymers with long-term stability for practical application.
- Despite the dominance of fluorinated monomers in top-performing polymers, we identified hundreds of novel, fluorine-free copolymers with strong predictive confidence, marking a significant step toward more sustainable materials.
- Future efforts will focus on expanding our dataset using natural language processing and advanced molecular modeling, paving the way for even more robust and generalizable models.

DECLARATIONS

Authors' contributions

Conceived and guided the work: Ramprasad, R.

Curated the training dataset from the literature: Schertzer, W., Shukla, S., Rafiq, R.

Designed, trained, and evaluated the machine-learning models: Schertzer, W., Shukla, S.

Generated the candidates, predicted their properties, and ranked them: Schertzer, W.

Provided insights into the theoretical and experimental details of the AEM systems: Lively, R. P., Sampath, J., Asl-Otmi, M.

Designed, trained and evaluated the machine learning models and provided insight into the theoretical and experimental details of the AEM systems: Sose, A.

All authors discussed the results and commented on the manuscript.

Availability of data and materials

The dataset used in this work and the property predictions for top-performing candidates are available on the [polyVERSE GitHub](#).

Financial support and sponsorship

This work was supported as part of the UNCAGE-ME, an Energy Frontier Research Center funded by the U.S. Department of Energy, Office of Science, Basic Energy Sciences at the Georgia Institute of Technology under award # DE-SC0012577.

Conflicts of interest

All authors declared that there are no conflicts of interest.

Ethical approval and consent to participate

Not applicable.

Consent for publication

Not applicable.

Copyright

© The Author(s) 2025.

REFERENCES

1. Dekel, D. R. Review of cell performance in anion exchange membrane fuel cells. *J. Power. Sources.* **2018**, *375*, 158-69. DOI
2. Mandal, M. Recent advancement on anion exchange membranes for fuel cell and water electrolysis. *ChemElectroChem* **2021**, *8*, 36-45. DOI
3. Hossen, M. M.; Hasan, M. S.; Sardar, M. R. I.; et al. State-of-the-art and developmental trends in platinum group metal-free cathode catalyst for anion exchange membrane fuel cell (AEMFC). *Appl. Catal. B. Environ.* **2023**, *325*, 121733. DOI
4. U.S. Department of Energy. Technical targets for proton exchange membrane electrolysis. Available from: <https://www.energy.gov/eere/fuelcells/technical-targets-proton-exchange-membrane-electrolysis>. [Last accessed on 10 Jan 2025].
5. Hossain, M. A.; Lim, Y.; Lee, S.; et al. Comparison of alkaline fuel cell membranes of random & block poly(arylene ether sulfone) copolymers containing tetra quaternary ammonium hydroxides. *Int. J. Hydrogen. Energy.* **2014**, *39*, 2731-9. DOI
6. Willdorf-Cohen, S.; Zhegur-Khais, A.; Ponce-González, J.; et al. Alkaline stability of anion-exchange membranes. *ACS. Appl. Energy. Mater.* **2023**, *6*, 1085-92. DOI PubMed PMC
7. Hydrogen and Fuel Cell Technologies Office multi-year program plan. 2024. Available from: <https://www.energy.gov/sites/default/files/2024-05/hfto-mypp-2024.pdf>. [Last accessed on 10 Jan 2025].
8. Raut, A.; Fang, H.; Lin, Y.; et al. Effect of membrane mechanics on AEM fuel cell performance. *Energy. Adv.* **2023**, *2*, 113-22. DOI
9. Lee, W. H.; Kim, Y. S.; Bae, C. Robust hydroxide ion conducting poly(biphenyl alkylene)s for alkaline fuel cell membranes. *ACS. Macro. Lett.* **2015**, *4*, 814-8. DOI PubMed
10. Douglin, J. C.; Singh, R. K.; Haj-Bsoul, S.; et al. A high-temperature anion-exchange membrane fuel cell with a critical raw material-free cathode. *Chem. Eng. J. Adv.* **2021**, *8*, 100153. DOI
11. Duan, Q.; Ge, S.; Wang, C. Y. Water uptake, ionic conductivity and swelling properties of anion-exchange membrane. *J. Power. Sources.* **2013**, *243*, 773-8. DOI
12. Liu, J.; Yan, X.; Gao, L.; et al. Long-branched and densely functionalized anion exchange membranes for fuel cells. *J. Membr. Sci.* **2019**, *581*, 82-92. DOI
13. Jheng, L.; Tai, C.; Hsu, S. L.; et al. Study on the alkaline stability of imidazolium and benzimidazolium based polyelectrolytes for anion exchange membrane fuel cells. *Int. J. Hydrog. Energy.* **2017**, *42*, 5315-26. DOI
14. Chu, J. Y.; Lee, K. H.; Kim, A. R.; Yoo, D. J. Improved electrochemical performance of composite anion exchange membranes for

- fuel cells through cross linking of the polymer chain with functionalized graphene oxide. *J. Membr. Sci.* **2020**, *611*, 118385. DOI
15. Al Otmí M, Lin P, Schertzer W, Colina CM, Ramprasad R, Sampath J. Investigating correlations in hydroxide ion transport in anion exchange membranes from atomistic molecular dynamics simulations. *ACS Appl. Polym. Mater.* **2024**, *6*, 11270-9. DOI
 16. Merle, G.; Wessling, M.; Nijmeijer, K. Anion exchange membranes for alkaline fuel cells: a review. *J. Membr. Sci.* **2011**, *377*, 1-35. DOI
 17. Hossain, M. M.; Hou, J.; Wu, L.; et al. Anion exchange membranes with clusters of alkyl ammonium group for mitigating water swelling but not ionic conductivity. *J. Membr. Sci.* **2018**, *550*, 101-9. DOI
 18. Zheng, Y.; Ash, U.; Pandey, R. P.; et al. Water uptake study of anion exchange membranes. *Macromolecules* **2018**, *51*, 3264-78. DOI
 19. Ramprasad, R.; Batra, R.; Piliand, G.; Mannodi-Kanakkithodi, A.; Kim, C. Machine learning in materials informatics: recent applications and prospects. *npj. Comput. Mater.* **2017**, *3*, 56. DOI
 20. Tran, H.; Gurnani, R.; Kim, C.; et al. Design of functional and sustainable polymers assisted by artificial intelligence. *Nat. Rev. Mater.* **2024**, *9*, 866-86. DOI
 21. Tran, H.; Shen, K.; Shukla, S.; Kwon, H.; Ramprasad, R. Informatics-driven selection of polymers for fuel-cell applications. *J. Phys. Chem. C.* **2023**, *127*, 977-86. DOI
 22. Xu, P. Y.; Zhou, K.; Han, G. L.; Zhang, Q. G.; Zhu, A. M.; Liu, Q. L. Fluorene-containing poly(arylene ether sulfone)s as anion exchange membranes for alkaline fuel cells. *J. Membr. Sci.* **2014**, *457*, 29-38. DOI
 23. Weiber, E. A.; Jannasch, P. Polysulfones with highly localized imidazolium groups for anion exchange membranes. *J. Membr. Sci.* **2015**, *481*, 164-71. DOI
 24. Wang, J.; Wang, J.; Li, S.; Zhang, S. Poly(arylene ether sulfone)s ionomers with pendant quaternary ammonium groups for alkaline anion exchange membranes: preparation and stability issues. *J. Membr. Sci.* **2011**, *368*, 246-53. DOI
 25. Wang, C.; Shen, B.; Xu, C.; Zhao, X.; Li, J. Side-chain-type poly(arylene ether sulfone)s containing multiple quaternary ammonium groups as anion exchange membranes. *J. Membr. Sci.* **2015**, *492*, 281-8. DOI
 26. Wang, C.; Xu, C.; Shen, B.; Zhao, X.; Li, J. Stable poly(arylene ether sulfone)s anion exchange membranes containing imidazolium cations on pendant phenyl rings. *Electrochim. Acta.* **2016**, *190*, 1057-65. DOI
 27. Vijayakumar, V.; Son, T. Y.; Kim, H. J.; Nam, S. Y. A facile approach to fabricate poly(2,6-dimethyl-1,4-phenylene oxide) based anion exchange membranes with extended alkaline stability and ion conductivity for fuel cell applications. *J. Membr. Sci.* **2019**, *591*, 117314. DOI
 28. Shen, K.; Zhang, Z.; Zhang, H.; Pang, J.; Jiang, Z. Poly(arylene ether ketone) carrying hyperquaternized pendants: preparation, stability and conductivity. *J. Power. Sources.* **2015**, *287*, 439-47. DOI
 29. Seo, D. W.; Hossain, M. A.; Lee, D. H.; et al. Anion conductive poly(arylene ether sulfone)s containing tetra-quaternary ammonium hydroxide on fluorenyl group for alkaline fuel cell application. *Electrochim. Acta.* **2012**, *86*, 360-5. DOI
 30. Prakash, O.; Bihari, S.; Keshav; Tiwari, S.; Prakash, R.; Maiti, P. Dehydrohalogenated poly(vinylidene fluoride)-based anion exchange membranes for fuel cell applications. *Mater. Today. Chem.* **2022**, *23*, 100640. DOI
 31. Lai, A. N.; Wang, L. S.; Lin, C. X.; et al. Benzylmethyl-containing poly(arylene ether nitrile) as anion exchange membranes for alkaline fuel cells. *J. Membr. Sci.* **2015**, *481*, 9-18. DOI
 32. He, Y.; Si, J.; Wu, L.; et al. Dual-cation comb-shaped anion exchange membranes: structure, morphology and properties. *J. Membr. Sci.* **2016**, *515*, 189-95. DOI
 33. Fang, J.; Shen, P. K. Quaternized poly(phthalazinone ether sulfone ketone) membrane for anion exchange membrane fuel cells. *J. Membr. Sci.* **2006**, *285*, 317-22. DOI
 34. Fang, J.; Lyu, M.; Wang, X.; Wu, Y.; Zhao, J. Synthesis and performance of novel anion exchange membranes based on imidazolium ionic liquids for alkaline fuel cell applications. *J. Power. Sources.* **2015**, *284*, 517-23. DOI
 35. Abuin, G. C.; Nonjola, P.; Franceschini, E. A.; Izraelevitch, F. H.; Mathe, M. K.; Corti, H. R. Characterization of an anionic-exchange membranes for direct methanol alkaline fuel cells. *Int. J. Hydrog. Energy.* **2010**, *35*, 5849-54. DOI
 36. Zhuo, Y. Z.; Lai, A. L.; Zhang, Q. G.; Zhu, A. M.; Ye, M. L.; Liu, Q. L. Enhancement of hydroxide conductivity by grafting flexible pendant imidazolium groups into poly(arylene ether sulfone) as anion exchange membranes. *J. Mater. Chem. A.* **2015**, *3*, 18105-14. DOI
 37. Zhu, L.; Yu, X.; Peng, X.; et al. Poly(olefin)-based anion exchange membranes prepared using Ziegler–Natta polymerization. *Macromolecules* **2019**, *52*, 4030-41. DOI
 38. Zhu, L.; Pan, J.; Christensen, C. M.; Lin, B.; Hickner, M. A. Functionalization of poly(2,6-dimethyl-1,4-phenylene oxide)s with hindered fluorene side chains for anion exchange membranes. *Macromolecules* **2016**, *49*, 3300-9. DOI
 39. Zhu, L.; Peng, X.; Shang, S.; et al. High performance anion exchange membrane fuel cells enabled by fluoropoly(olefin) membranes. *Adv. Funct. Mater.* **2019**, *29*, 1902059. DOI
 40. Zhu, L.; Pan, J.; Wang, Y.; Han, J.; Zhuang, L.; Hickner, M. A. Multication side chain anion exchange membranes. *Macromolecules* **2016**, *49*, 815-24. DOI
 41. Zhang, M.; Shan, C.; Liu, L.; et al. Facilitating anion transport in polyolefin-based anion exchange membranes via bulky side chains. *ACS Appl. Mater. Interfaces.* **2016**, *8*, 23321-30. DOI
 42. Zhang, M.; Liu, J.; Wang, Y.; An, L.; Guiver, M. D.; Li, N. Highly stable anion exchange membranes based on quaternized polypropylene. *J. Mater. Chem. A.* **2015**, *3*, 12284-96. DOI
 43. Tanaka, M.; Fukasawa, K.; Nishino, E.; et al. Anion conductive block poly(arylene ether)s: synthesis, properties, and application in

- alkaline fuel cells. *J. Am. Chem. Soc.* **2011**, *133*, 10646-54. DOI
44. Si, J.; Lu, S.; Xu, X.; Peng, S.; Xiu, R.; Xiang, Y. A gemini quaternary ammonium poly (ether ether ketone) anion-exchange membrane for alkaline fuel cell: design, synthesis, and properties. *ChemSusChem* **2014**, *7*, 3389-95. DOI
 45. Pham, T. H.; Olsson, J. S.; Jannasch, P. N-spirocyclic quaternary ammonium ionenes for anion-exchange membranes. *J. Am. Chem. Soc.* **2017**, *139*, 2888-91. DOI PubMed
 46. Park, E. J.; Kim, Y. S. Quaternized aryl ether-free polyaromatics for alkaline membrane fuel cells: synthesis, properties, and performance - a topical review. *J. Mater. Chem. A* **2018**, *6*, 15456-77. DOI
 47. Pan, J.; Zhu, L.; Han, J.; Hickner, M. A. Mechanically tough and chemically stable anion exchange membranes from rigid-flexible semi-interpenetrating networks. *Chem. Mater.* **2015**, *27*, 6689-98. DOI
 48. Pan, J.; Li, Y.; Han, J.; et al. A strategy for disentangling the conductivity–stability dilemma in alkaline polymer electrolytes. *Energy. Environ. Sci.* **2013**, *6*, 2912-5. DOI
 49. Miyake, J.; Fukasawa, K.; Watanabe, M.; Miyatake, K. Effect of ammonium groups on the properties and alkaline stability of poly(arylene ether) based anion exchange membranes. *J. Polym. Sci. Part. A. Polym. Chem.* **2014**, *52*, 383-9. DOI
 50. Lin, B.; Qiu, L.; Qiu, B.; Peng, Y.; Yan, F. A soluble and conductive polyfluorene ionomer with pendant imidazolium groups for alkaline fuel cell applications. *Macromolecules* **2011**, *44*, 9642-9. DOI
 51. Li, Y.; Jackson, A. C.; Beyer, F. L.; Knauss, D. M. Poly(2,6-dimethyl-1,4-phenylene oxide) blended with poly(vinylbenzyl chloride)-*b*-polystyrene for the formation of anion exchange membranes. *Macromolecules* **2014**, *47*, 6757-67. DOI
 52. Li, X.; Nie, G.; Tao, J.; Wu, W.; Wang, L.; Liao, S. Assessing the influence of side-chain and main-chain aromatic benzyltrimethyl ammonium on anion exchange membranes. *ACS. Appl. Mater. Interfaces.* **2014**, *6*, 7585-95. DOI PubMed
 53. Li, X.; Cheng, S.; Wang, L.; et al. Anion exchange membranes by bromination of benzylmethyl-containing poly(arylene ether)s for alkaline membrane fuel cells. *RSC. Adv.* **2014**, *4*, 29682-93. DOI
 54. Li, N.; Yan, T.; Li, Z.; Thurn-Albrecht, T.; Binder, W. H. Comb-shaped polymers to enhance hydroxide transport in anion exchange membranes. *Energy. Environ. Sci.* **2012**, *5*, 7888. DOI
 55. Lai, A. N.; Wang, L. S.; Lin, C. X.; et al. Phenolphthalein-based poly(arylene ether sulfone nitrile)s multiblock copolymers as anion exchange membranes for alkaline fuel cells. *ACS. Appl. Mater. Interfaces.* **2015**, *7*, 8284-92. DOI
 56. Kostalik, H. A.; Clark, T. J.; Robertson, N. J.; et al. Solvent processable tetraalkylammonium-functionalized polyethylene for use as an alkaline anion exchange membrane. *Macromolecules* **2010**, *43*, 7147-50. DOI
 57. Hibbs, M. R.; Fujimoto, C. H.; Cornelius, C. J. Synthesis and characterization of poly(phenylene)-based anion exchange membranes for alkaline fuel cells. *Macromolecules* **2009**, *42*, 8316-21. DOI
 58. Hibbs, M. R.; Hickner, M. A.; Alam, T. M.; McIntyre, S. K.; Fujimoto, C. H.; Cornelius, C. J. Transport properties of hydroxide and proton conducting membranes. *Chem. Mater.* **2008**, *20*, 2566-73. DOI
 59. Guo, D.; Lai, A. N.; Lin, C. X.; Zhang, Q. G.; Zhu, A. M.; Liu, Q. L. Imidazolium-functionalized poly(arylene ether sulfone) anion-exchange membranes densely grafted with flexible side chains for fuel cells. *ACS. Appl. Mater. Interfaces.* **2016**, *8*, 25279-88. DOI
 60. Ge, Q.; Ran, J.; Miao, J.; Yang, Z.; Xu, T. Click chemistry finds its way in constructing an ionic highway in anion-exchange membrane. *ACS. Appl. Mater. Interfaces.* **2015**, *7*, 28545-53. DOI
 61. Kuenneth, C.; Schertzer, W.; Ramprasad, R. Copolymer informatics with multitask deep neural networks. *Macromolecules* **2021**, *54*, 5957-61. DOI
 62. Bishnoi, S.; Singh, S.; Ravinder, R.; et al. Predicting Young's modulus of oxide glasses with sparse datasets using machine learning. *J. Non. Cryst. Solids.* **2019**, *524*, 119643. DOI
 63. Bishnoi, S.; Ravinder, R.; Grover, H. S.; Kodamana, H.; Krishnan, N. M. A. Scalable Gaussian processes for predicting the optical, physical, thermal, and mechanical properties of inorganic glasses with large datasets. *Mater. Adv.* **2021**, *2*, 477-87. DOI